Influence of process variables on foaming ability of surfactants: Experimental study and dimensional analysis

Rémy Bois, Océane Adriao, Guillaume Delaplace, Isabelle Pezron, Alla Nesterenko, Elisabeth Van-Hecke

1   **Influence of process variables on foaming ability of surfactants: experimental study and**

2   **dimensional analysis**

3   Rémy Bois[1]*, Océane Adriao[1], Guillaume Delaplace[2], Isabelle Pezron[1], Alla Nesterenko[1],

4   Elisabeth van-Hecke[1]

[1]*Sorbonne Universités, Université de Technologie de Compiègne, ESCOM, EA 4297 TIMR, rue du Dr Schweitzer, 60200 Compiègne, France*

5   [2]*Unité Matériaux et Transformations (UMET) – UMR 8207, INRA, Team PIHM, 369 rue*

6   *Jules Guesde, 59650 Villeneuve d'Ascq, France*

7   * Corresponding author: alla.nesterenko@utc.fr

8

9   **Abstract**

10 By applying the dimensional analysis approach to a lab-scale stirred tank process, the

11 influence of process parameters on the foamability of three model surfactants: SLES, Tween

12 20 and Brij L23 is investigated and modelled. For validation of process law, the theoretical

13 approach is complemented with an experimental work varying process parameters such as

14 agitator rotational speed rate (N), mixing time (t_m) and bottom clearance (C_b). The foam rate

15 of expansion of surfactant solutions is correlated with success to two dimensionless numbers:

16 the Reynolds number and the mixing time number. Reynolds number is observed as mainly

17 governing the amount of formed foam. A clear difference between the intermediate flow

18 regime (Re < 10^5) and the turbulent one (Re > 10^5) is observed leading to a different process

19 law for each regime. Master curves are finally drawn and can be used for helping to predict

20 final foam volumes in the studied experimental domain according to both dimensionless

21 numbers.

22

23   *Keywords: foaming, dimensional analysis, Reynolds number, surfactant, process, mechanical*

24   *stirring*

1. Introduction

Numerous technics exist to disperse a gaseous phase into a liquid phase and to generate a foam (Pugh 2016): air incorporation by mechanical stirring (surface aeration), growing bubbles by gas injection, nucleation or chemical reactions. Among them, bubble formation and break-up under shear has been widely studied. In case of surface aeration with mechanical rotating devices, introduction of gas is driven by process parameters such as the rotational speed of the agitator, and is facilitated by the reduced pressure in regions close to rotating blades, induced by the liquid motion. The foaming solution and the gas are strongly sheared to create foam of generally submillimetric bubbles (Drenckhan et al. 2015). Mechanisms of small bubbles formation have been well described in the literature (Müller et al. 2008, Drenckhan et al. 2015). During the first steps of agitation, air at the liquid surface is brought into the solution and enables formation of large bubbles. Under shear, bubbles are then deformed into an elongated shape whose size depends on fluid properties, on the ability of surface agent (surfactants, proteins, polymers) to stabilize the interface, and on imposed shear flow (Stone 2003, Cristini et al. 2004). At a critical size, the bubble breaks and forms smaller bubbles (Müller et al. 2008).

The challenging issue concerning these mechanical devices is generally to obtain foams with desired bubble size and gas fraction, all along with energy efficiency (low power consumption). Three main types of mechanical agitators are often studied when foam generation is considered. The first of them is the planetary mixer, or commonly called kitchen blender, broadly used in the whipping of food foams (Camacho et al. 1998, Massey et al. 2001, Jakubczyk et al. 2006, Müller et al. 2007, Delaplace et al. 2012, Chesterton et al. 2013). Such device allows obtaining very small bubbles (diameters between 0.01 mm and 1 mm), leading to the white aspect of the final foam. Continuous rotor-stator mixers are also found to be efficient for foam generation (Kroezen et al. 1988, Hanselmann et al. 1998, Müller-Fischer

et al. 2005). In such devices, the foaming process is carried out in a relatively small mixing space between a rotor and a stator, both with pins, and gas injection is continuous and controlled. The optimal design of the set is largely discussed, depending on the fluids involved. Finally, stirred tanks with various impellers and coupled or not to gas sparging are also used to produce a foam (Hu et al. 2003, Indrawati et al. 2008, Wu et al. 2012, Celani et al. 2018). In such devices, the impeller type (blade, turbine or propeller) and size greatly influence the fluid flow pattern and so the foaming properties of the solution.

The influence of mechanical agitation process parameters in stirred vessels and the understanding of mechanisms for foam formation have been discussed for years. The literature has shown that the bubble size is a particular foam property and as a consequence is often employed as a target variable for studying the effect of different process parameters. It was shown for various kinds of foams that average bubble diameter generally decreases with an increase of agitation speed due to higher shear and turbulence (Machon et al. 1997, Hu et al. 2003, Indrawati et al. 2008, Wu et al. 2012, Celani et al. 2018). However, Samaras et al. (Samaras et al. 2014) found that in the presence of surfactant solutions, bubble size was not affected by agitation speed. Furthermore, the bubble size can reach a constant value at high agitation speed as well as at long enough residence time which has been explained by a dynamic equilibrium between breakage and coalescence (Hu et al. 2003, Wu et al. 2012). On the contrary, other study demonstrated no influence of coalescence/breakage phenomena from their observed data (Samaras et al. 2014). In addition, some of the authors highlighted that foam bubble size was mainly affected by the volumetric energy input. The energy involved is related to different variables, such as for example rotor speed, mixing time, fluid viscosity and density (Delaplace et al. 2015).

Otherwise, analysis of scientific papers dealing with foaming reveals that properties other than bubble size are used to characterize foaming properties of a surfactant solution. Among

others, one can distinguish foaming capacity, sometimes expressed as gas hold-up or overrun. All those terms are indicators of final amount (volume or height) of foam generated. The amount of produced foam is related to process variables for mechanical agitation method in several studies (Delaplace et al. 2012, Samaras et al. 2014, Celani et al. 2018). An increase of foam volume is observed when increasing rotational speed (Samaras et al. 2014, Celani et al. 2018). Indrawati et al. (Indrawati et al. 2008) used foam density as indicator of foamability and found a decrease of density with increasing speed rate which is in agreement with other studies (Samaras et al. 2014, Celani et al. 2018).

Besides process parameters, the foaming behavior of amphiphilic molecule is governed by its chemical structure, adsorption properties and solution characteristics. In foaming processes, the increase in viscosity of aqueous solution usually leads to the slowdown of foam destabilization, helping reduce bubble size (Ding et al. 2019, Santini et al. 2019), prevent liquid drainage and bubble coalescence (Mohanan et al. 2020, Zhu et al. 2021). Regarding the amount of produced foam, there is no general tendency relating this parameter with viscosity of solution or with equilibrium surface tension of surfactant at CMC (γ_{CMC}). In the case of protein stabilized foams, viscosity and foam amount are generally increased for higher pH values (Mohanan et al. 2020). Kanokkarn et al (Kanokkarn et al. 2017) demonstrated that this trend is strongly affected by the surfactant structure variation: for a series of methyl ester sulfonate with different alkyl chain length, foamability increases for higher γ_{CMC} values, whereas for a series of polyoxyethylated dodecyl alcohol with variable head group size, foamability decreases when γ_{CMC} raises.

Besides these studies on foaming processes, an important use of modelling by dimensional analysis have emerged to further investigate the mixing processes (Zlokarnik 1998, Delaplace et al. 2015) since the pioneer work of Nagata et al. (Nagata et al. 1957). This approach brought better apprehension of mixing mechanisms taking place in a batch reactor, is still

100 applied nowadays and allowed scaling rules for design of mixing operations (Hsu et al. 1996,

101 Manjula et al. 2010, André et al. 2012, Pradilla et al. 2015). Modelling mixing operations

102 through dimensional analysis has the advantage not to be constrained to a specific type of

103 agitated media (i.e monophasic liquid, liquid/liquid dispersion, gas/liquid dispersion,

104 powders) or to be applied only for classical batch mixing systems (i.e with an agitator rotating

105 around a vertical axis centrally located in the tank). For example, Delaplace et al. (Delaplace

106 et al. 2018) applied the approach for the homogenization of Newtonian miscible liquids in soft

107 elastic reactor that induces mixing by vibration of the tank wall while André et al. (André et

108 al. 2012) performed it for the homogenization of powders agitated with a planetary mixer.

109 The effect of emulsification process parameters and development of quantitative correlation

110 with microspheres size were also investigated by this as well as the scale-up prediction (Hsu

111 et al. 1996). Otherwise, this method of modelling was applied for studying foam elaboration

112 in a continuous mixing equipment (Mary et al. 2013) and spray drying of maltodextrin

113 solutions (Lachin et al. 2020).

114 From the only analysis of the exhaustive works of Delaplace & al. dealing with modelling

115 mixing operations by dimensional analysis, it appears that a lot of dimensional target

116 variables can be chosen to describe the evolution of the mixing system and relate them to the

117 causal dimensional physical quantities responsible for the evolution of the mixing system

118 through process relationship: heat transfer coefficient (Delaplace et al. 2001), power

119 consumption (Delaplace et al. 2005, Delaplace et al. 2007), mixing time (Delaplace et al.

120 2007), volumetric gas–liquid mass transfer coefficient (Hassan et al. 2012), gas hold up

121 (Delaplace et al. 2012). Moreover, using dimensionless numbers can be interesting for

122 scaling-up processes. Indeed, clear guidelines exist to evaluate whether a condition of

123 similarity occurs between the model and the prototype. These conditions of similarity require

124 the equality of the numerical value of each dimensionless number involved on both scales as

125   remembered in lots of books on the subject (Zlokarnik 1998, White 2001, Szirtes et al. 2007,

126   Delaplace et al. 2015). In this sense, dimensional analysis allows us to dispose of a scientific

127   frame for scaling-up.

128   Beyond the fact that dimensional analysis can provide scaling laws, modelling by dimensional

129   analysis is ever interesting at lab-scale for discriminating different surfactants abilities as

130   reducing the number of experiments for obtaining process relationship. Moreover, in depth

131   understanding the relation between the parameters responsible for foam formation process and

132   the amount of produced foam has direct relevance for the choice of surfactant. At this stage,

133   to be in ability to select surfactants for foaming formulation requires additional and accurate

134   knowledge about the specific role played by all physical quantities (arising from process,

135   geometry of mixing equipment and agitated media) involved in the foaming operation.

136   Up to date, only a few scientific studies have focused on dimensional analysis of foaming

137   process in agitated vessels. Machon et al. (Machon et al. 1997) summarized the basis for

138   dimensional correlations between bubble size and process-product parameters considering

139   bubble break-up processes on the one hand and coalescence processes on the other hand.

140   Those correlations mainly involve rotation speed, impeller diameter, power input, liquid

141   volume, density, viscosity and surface tension and foam volume. Smith (Smith 1992) gathered

142   data from various authors and showed that in many cases, gas holdup is correlated with

143   sufficient accuracy in a monomial form to Reynolds number (Re), Froude number (Fr), gas

144   flow number (Flg), and a geometrical dimensionless number characterizing the position of the

145   impeller in the tank. However this single monomial relationship does not take into account

146   mixing time nor surfactants solution properties like surface tension. The same remark can be

147   done from the work of Delaplace et al. (Delaplace et al. 2012) with planetary mixer since only

148   one recipe was carried out as the foaming solution, even if in this case the mixing time effect

149   was discussed.

In the present study, a dimensional analysis of a lab-scale stirred tank process is carried out in view of establishing a causal relationship between foaming properties of surfactants solutions, especially their foaming ability, and process variables. This theoretical approach is complemented with an experimental work varying process parameters and measuring the evolution of foam height with mixing time in order to validate the obtained semi-empirical correlations. Three model surfactants solutions at their critical micellar concentration (CMC) were foamed. Such a study aims at a better understanding of which of the physical phenomena mainly control foam formation in a classic mechanical agitator.

Nomenclature

Ca	Capillary number	R_e	Reynolds number
C_b	bottom clearance of the agitator (m)	T	tank diameter (m)
d	agitator diameter (m)	t_m	mixing time (s)
Fr	Froude number	W_e	Weber number
g	constant of gravity (m.s^{-2})	γ	surface tension
H_F	height of foam generated (m)	η	liquid Newtonian viscosity (Pa.s)
H_L	liquid height in the tank (m)	ρ	liquid density (kg.m^{-3})
N	rotational speed of agitator (s^{-1})	Θ_m	mixing time number

2. Experimental setup

2.1. Surfactants solutions

Tween 20 (> 97 %, M_w=1227.5 g.mol^{-1}), Brij L23 (> 98 %, M_w=1198 g.mol^{-1}) were purchased from Sigma-Aldrich and used without further purification. SLES (M_w=370 g.mol^{-1}) was provided from THOR Personal Care SAS (La Croix Saint-Ouen, France) as 27 wt % aqueous solution (Texapon® NSO UP). Ultrapure water with a resistivity of 18.2 MΩ.cm

167   produced by a PureLab Classic purification chain (Elga/Veolia, Wissous, France) was used

168   for all analysis. Model solutions at different concentrations were prepared by dissolving a

169   known quantity of pure surfactant in ultrapure water.

170

171   *2.2. Critical micellar concentration determination*

172   The measurement of surface tension at equilibrium (γ_{eq}) were obtained using K100 Krüss

173   tensiometer (Hamburg, Germany) equipped with a Wilhelmy platinum plate (length 10 mm,

174   width 19.9 mm, thickness 0.2 mm). The tensiometer operates by holding a plate in a fixed

175   vertical position attached to a microbalance. The microbalance measures the force acting on

176   the plate, which is used for the calculation of surface tension. The resolution of the

177   microbalance for all measurements is of 10 µg, which corresponds to a resolution of

178   0.0024 mN.m^{-1} on the surface tension scale. The sample solution was put in a glass vessel

179   surrounded by a circular thermostated system maintained at 25 ± 1°C. Prior to each

180   determination, the plate was rinsed with ethanol and water, and burnt to red-hot conditions in

181   a blue flame to ensure perfect wetting (zero contact angle). The measurement of surface

182   tension at the air/liquid interface was carried out by submerging a Wilhelmy plate in the

183   solution during several minutes (time required to reach an equilibrium surface tension (γ_{eq}).

184   All measurements were repeated at least three times. The Critical Micellar Concentration

185   (CMC) of each surfactant was determined from the break point of concentration-surface

186   tension curve. CMC values obtained are listed below and were similar to values from

187   literature:

188   -   SLES: 0.5 mM (Rosen et al. 1996)

189   -   Tween 20: 0.04 mM (Patist et al. 2000)

190   -   Brij L23: 0.07 mM (Patist et al. 2000, Wang et al. 2005)

191

2.3. Foaming method

The foaming experiments were performed with surfactants solutions at critical micellar concentration (CMC). As CMC of all studied solutions was lower than 1mM, density (ρ) and viscosity (η) could be assumed constants and equal to those of water: 10^3 kg.m^{-3} and 0.001 kg.m^{-1}.s^{-1} respectively. A mechanical stirrer (IKA Eurostar20 high speed digital, IKA Labortechnik, Staufen, Germany) equipped with a 4-bladed stirring element R1342 (diameter: 5 cm) was used for the present study. 100 mL of a fresh solution were placed in a 600 mL beaker (diameter of beaker: 9 cm; initial liquid height, H_L: 2.8 cm). Stirrer was fixed at different heights (1 – 2.8 cm) from beaker bottom. Agitation was applied at various speeds (70 – 6000 rpm) for different mixing times (30 – 300 s). Foaming ability of surfactant was characterized by measuring foam height (H_F) directly after the end of agitation process. Measurement of foam heights was realized visually from the graduated beaker. Foam rate of expansion expressed as the ratio of generated foam height over initial liquid height (H_F/H_L) was chosen as target dimensionless variable. Experiments were carried out in triplicates.

3. Dimensional analysis

The dimensional analysis of mechanical stirring process applied to foam formation was performed according to the methodology described by Delaplace et al. (Delaplace et al. 2015).

3.1. Physical variables involved in the process

Experimental variables that might influence the foam height (H_F) were identified, as a first step of dimensional analysis. One can distinguish four kinds of physical quantities involved in the process as illustrated in Fig. 1.

- Parameters related to surfactant solution: density (ρ), viscosity (η) and equilibrium surface tension (γ_{eq});

217   -   Process parameters: mixing time (t_m) and agitator rotational speed rate (N);

218   -   Geometrical parameters, giving information related to the domain of flow application:

219   tank diameter (T), stirrer diameter (d), initial liquid height (H_L) and bottom clearance

220   (C_b);

221   -   Boundary conditions applied to the studied mixing system: here, gravitational

222   acceleration (g) is the only boundary condition and, as explained in numerous articles

223   dealing with modelling by dimensional analysis, it should not be omitted even if this

224   physical dimensional quantity is in fact a dimensional constant in the study (Zlokarnik

225   1998, White 2001, Szirtes et al. 2007, Delaplace et al. 2015).

226   Thus, the foam height can be described as a function of all those physical quantities in a so-

227   called process law, as expressed in Eq. 1.

228
$$H_F = f_1(\rho, \gamma_{eq}, \eta, N, t_m, T, d, H_L, C_b, g) \quad \text{Eq. 1}$$

229

230   *3.2. Dimensionless numbers involved in the process*

231   All variables can be expressed according to three basic dimensions: time, length and mass. A

232   physical quantity (H_F) that is a function of ten others described by three fundamental

233   dimensions (mass, time, length) can be described by a new function of 7 dimensionless

234   numbers (Delaplace et al. 2015). A dimensional analysis enables to obtain such numbers as

235   indicated in the Buckingham π theorem (Zlokarnik 1998, White 2001, Szirtes et al. 2007,

236   Delaplace et al. 2015). Such set of dimensionless numbers, also called π-numbers, can be

237   obtained by:

238   Step 1: Listing dimensions of all variables.

239   Step 2: Choosing a set of repeated variables, called the base. The repeated variables

240   should be dimensionally independent and covering all the dimensions of the

241   dimensional variables encountered in the studied system. The choice of the base is

242   multiple and up to the user.

243   Step 3: Dividing each non-repeated variable by a product of repeated variables raised to

244   various exponent to obtain each dimensionless number. Algebraically, it consists to find

245   the exponents which make the product dimensionless.

246   Step 4: Rearranging the dimensionless numbers by raising it to any power and

247   multiplying it by other dimensionless numbers raised to different power.

248   Recombinations are possible and let the user find different set of π-numbers for a given

249   studied system The most common reasons associated to recombinations are i) to give

250   rise to common dimensionless numbers ii) to eliminate a physical quantity of a

251   dimensionless number in order to obtain a new dimensionless number independent of

252   this physical quantity .

253 The reader must retain that the choice of the base and rearrangements are multiple and up to

254 the user. Nevertheless, these choices will not affect the content of the data but only the form

255 of their presentation. These common 4 steps of modelling by dimensional analysis for

256 constructing a set of dimensionless numbers are mathematically explained and justified in

257 numerous books in which the reader can refer whether he would like to go further (Zlokarnik

258 1998, White 2001, Szirtes et al. 2007, Delaplace et al. 2015) so we will not detail them here in

259 depth.

260 In the following section, we will use this rule allowed by dimensional analysis to illustrate

261 and discuss particulate effects of the results. For our case, choosing the base (ρ, N, H_L) leads

262 to a set of seven dimensionless numbers for explaining the chosen dimensionless target

263 variable, H_F/H_L, also known as the foam rate of expansion, as follows:

264     $$\frac{H_F}{H_L} = f_2(\pi_1 = \frac{\eta}{\rho.N.H_L^2}, \pi_2 = \frac{\gamma_{eq}}{\rho.N^2.H_L^3}, \pi_3 = \frac{g}{N^2.H_L}, N.t_m, \pi_4 = \frac{d}{H_L}, \frac{T}{H_L}, \frac{C_b}{H_L}) \quad \text{Eq. 2}$$

265   Rearranging leads to a set of seven dimensionless numbers, including Reynolds, Froude and

266   Capillary numbers and mixing time number:

267         $\frac{H_F}{H_L} = f_3 (Re = \pi_1^{-1}.\pi_4^2, Ca = \pi_1^{-1}.\pi_4.\pi_2, Fr = \pi_3^{-1}.\pi_4.\pi_2, \Theta_m, \frac{d}{H_L}, \frac{T}{H_L}, \frac{C_b}{H_L})$ Eq. 3

268   with, $Re = \frac{\rho.N.d^2}{\eta}$, the Reynolds number, $Ca = \frac{\eta.N.d}{\gamma_{eq}}$, the Capillary number, $Fr = \frac{N^2.d}{g}$, the

269   Froude Number, and $\Theta_m = N.t_m$, the mixing time number.

270   Each dimensionless number appearing in Eq. 3 is a measure of the non-repeated variables,

271   respectively (liquid height, viscosity, equilibrium surface tension, gravitational acceleration,

272   agitator diameter, tank diameter, bottom clearance) and has consequently a precise physical

273   meaning. For instance, Reynolds number represents the ratio of inertial stress over viscous

274   stress; Capillary number is defined by the ratio of viscous stress over interfacial stress and

275   account for the effect of surface tension. Finally, the Froude number is the ratio of the inertial

276   force divided by gravitational force. This number is supposed to describe how the liquid free

277   surface is deformed and how the vortex rise when the impeller rotational speed increases. Θ_m

278   represents the number of revolutions achieved by the agitator for obtaining the given height of

279   foam and measures the effect of time on dynamic foam process.

280   Rearrangement of Eq. 3 could be performed in order that impeller rotational speed is involved

281   only in one dimensionless number. For example, replacing Froude number, Fr, by $Fr^{-1}Re^2$,

282   allows appearing another well-known dimensionless number: the Galilei number, Ga. The

283   Galilei number $(= \frac{d^3.g.\rho^2}{\eta})$ also measures gravitational effect but this time independently of

284   impeller rotational speed. In the same way, it is possible to replace the capillary number Ca by

285      $Ca^* = Ca\, Re^{-1}$ in order that the new dimensionless number, Ca^*, measuring γ_{eq} effect,

286   becomes independent of the agitator rotational speed $(Ca^* = \frac{\eta^2}{\rho.d.\gamma_{eq}})$.

287   Consequently, the following π-spaces can be used indifferently to represent and to discuss the

288   results about foaming process in batch reactor:

13

289
$$\frac{H_F}{H_L} = f_4\left(Re, Ca, Fr, \Theta_m, \frac{d}{H_L}, \frac{T}{H_L}, \frac{C_b}{H_L}\right) \quad \text{Eq. 4 (idem Eq.3)}$$

290
$$\frac{H_F}{H_L} = f_5\left(Re, Ca, Ga, \Theta_m, \frac{d}{H_L}, \frac{T}{H_L}, \frac{C_b}{H_L}\right) \quad \text{Eq. 5}$$

291
$$\frac{H_F}{H_L} = f_6\left(Re, Ca^*, Ga, \Theta_m, \frac{d}{H_L}, \frac{T}{H_L}, \frac{C_b}{H_L}\right) \quad \text{Eq. 6}$$

292

293   As mentioned above, much more π-spaces exist and could be built but only the 3 above ones

294   will be used latter in our discussion.

295

296   *3.3. Establishment of the process relationship relevant to the study*

297   For the present study, as some dimensional variables are held constant during the

298   experimental runs, several levels of simplification were possible in Eq.4 to Eq.6. Tank

299   diameter (T) and stirrer diameter (d) were kept constant, as well as the initial height of

300   surfactant solution (H_L). Therefore, T/H_L and d/H_L remained at constant values. Furthermore,

301   as surfactant solutions were studied at a concentration equal to their CMC (CMC < 1 mM for

302   the three surfactants), density and viscosity were assumed constants and equal to those of pure

303   water. Thereby, Galilei number becomes constant. Consequently, with regards to the specific

304   experimental program applied here, the influence of some dimensionless numbers appearing

305   in Eq.4 to Eq.6 cannot be studied and the reduced π-spaces are now given in Eq. 7 and Eq.8.

306
$$\frac{H_F}{H_L} = f_7\left(Re, Ca, \Theta_m, \frac{C_b}{H_L}\right) \quad \text{Eq. 7}$$

307
$$\frac{H_F}{H_L} = f_8\left(Re, Ca^*, \Theta_m, \frac{C_b}{H_L}\right) \quad \text{Eq. 8}$$

308   Dimensional analysis and specific experimental program give rise to reduced π-spaces which

309   may explain the evolution of the target variable (here the amount of foam). However,

310   dimensional analysis doesn't indicate the mathematical form of the process relationship

311   correlating the dimensionless numbers relative to the causes, with the target dimensionless

312 number ($= \frac{H_F}{H_L}$). Since a monomial form function (like Eq. 9) can display a wide spectrum of

313 plots, depending on the values of unknowns ($Const$, a, b, c and d appearing in Eq.9), and

314 minimizes the number of unknowns to be identified, this mathematical equation is often

315 considered to adjust to experimental data (White 2001, Szirtes et al. 2007, Delaplace et al.

316 2015). So this simple form of mathematical equation was attempted in our study for

317 correlating foaming ability of surfactants solutions as a function of process variables.

318 Monomial form applied to Eq. 8 gives Eq. 9:

319 $$\frac{H_F}{H_L} = Const. \, \mathrm{Re}^a \, \mathrm{Ca^*}^b \Theta_m{}^c \left(\frac{C_b}{H_L}\right)^d \quad (Const, \text{ a, b, c and d being constants}) \quad \text{Eq. 9}$$

320 Adjustment of this model to experimental data was performed using the least squares method,

321 allowing to obtain the coefficients ($Const$, a, b, c and d). To evaluate model performance,

322 correlation coefficient (R^2) and mean absolute error (MAE, Eq.10) were calculated.

323 $$\mathrm{MAE} = \frac{1}{n} \sum_{i=1}^{n} |y - \hat{y}| \quad \text{Eq. 10}$$

324 with n, the number of experiments, y and $\hat{y}$ the experimental and predicted expansion rate,

325 respectively.

326

4. Results and discussion

328 *4.1. Influence of process variables on foaming ability :case of SLES solution*

329 Foaming experiments were carried out for SLES solutions at CMC, by varying the agitation

330 speed (5 levels), mixing time (4 levels) and bottom clearance (3 levels), into 38 assays as

331 reported in Table 1. The results are illustrated in Fig. 2 and Fig. 3.

332 Fig. 2 focuses on the influence of bottom clearance through its associated dimensionless

333 number (C_b/H_L). A C_b/H_L value of 1 means that the agitator was placed at liquid-air interface,

334 C_b/H_L values of 0.2 and 0.5 correspond to the agitator immersed into surfactant solution. For a

335 same agitation process, i.e. fixed time and speed of agitation, Fig. 2 shows that similar rates of

336   expansion were obtained whatever the bottom clearance. Even when the agitator is entirely

337   immersed in the solution, agitation speed was sufficient to generate enough air-liquid

338   interface and create bubbles. This result shows that the corresponding dimensionless number

339   (C_b/H_L) involved in Eq. 9 has finally little influence on final foam amount.

340   The influence of Reynolds number on foam expansion rate at $C_b/H_L=1$ is shown in Fig. 3a. A

341   significant increase of the foam rate of expansion (x10 approximately) with increasing the

342   Reynolds number from 3.10^4 to 24.10^4 is observed. A maximum of H_F/H_L is observable at

343   Reynolds values between 10.10^4 and 15.10^4, for all investigated mixing time values (Fig. 3a).

344   A value of Re close to 10.10^4 is usually associated with a transition from intermediate flow

345   regime to turbulent regime for stirred tanks of various configurations (Medek et al. 1979, Hall

346   2018). This transition might explain a maximum in final foam volumes. In the intermediate

347   regime, an increase of rotation speed facilitates incorporation of air within the liquid,

348   producing more foam. At higher agitation speeds corresponding to turbulent regime, the

349   mixed system probably undergoes too strong turbulence that would induce foam collapse.

350   Thus, the phenomenon of bubbles breakup occurs faster than foam generation, leading to a

351   stagnation then a decrease in height of formed foam.

352   As shown in Fig. 3b, the mixing time number (Θ_m) has also a significant influence on final

353   foam height. Extending the mixing time number usually allows producing higher amount of

354   foam, by increasing the number of exchanges between gas and liquid, which facilitates

355   creation of interfaces. Furthermore, the obtained results also demonstrated the presence of a

356   plateau for foam volumes. At a certain mixing time number, expansion rate remains constant,

357   at a value that depends on the agitation speed. This result can be put in regards with Bikerman

358   work (Bikerman 1973) in case of a sparging method (gas injection through a frit): the foams

359   reach a plateau value called "foaminess" that depends on gas flow rate. At relatively low flow

360   rates, the amount of formed foam increases proportionally to gas superficial velocity. One can

361   suppose that the same observation is transposable in the intermediate regime (Re < 10^5) for

362   the present study. From Fig. 3, both mixing time and agitation speed play major roles for the

363   formation of foam. For example, considering Θ_m close to 3500, result of the experiment could

364   be significantly different: H_F/H_L of 0.58 for trial 10 (700 rpm for 300 s) and H_F/H_L of 2.97 for

365   trial 22 (3360 rpm for 30 s).

366

367   *4.2. Fitting the process law to experimental data: case of SLES solution*

368   Considering the only surfactant SLES, at CMC, it is possible to further simplify the generic

369   monomial process law (Eq. 9) since Ca* (= $Ca\,Re^{-1} = \dfrac{\eta^2}{\rho.d.\gamma_{eq}}$) is constant (γ_{eq} being

370   constant here). The form of the resulting process law thus becomes as follows:

371    $$\frac{H_F}{H_L} = Const.\,Re^a \Theta_m{}^c \left(\frac{C_b}{H_L}\right)^d \quad \text{Eq. 11}$$

372   Since two regimes of flow were clearly identified as having different consequences on foam

373   expansion rate (Fig. 3a), each of them was considered separately. Firstly, the intermediate

374   flow regime (10^4 < Re < 10^5) was considered. The first 20 lines from Table 1 were used to

375   identify the four coefficients: $Const$, a, c and d in that domain. According to the Table 1, it

376   should be noticed that the maximal studied Θ_m was 10^4 in that Re range. Calculations lead to

377   the process relationship expressed in Eq. 12. Model data were in good agreement with

378   experimental points, as presented in Fig. 4a ($R^2 = 0.95$).

379    $$\frac{H_F}{H_L} = 10^{-7} Re^{1.09} \Theta_m{}^{0.57} \left(\frac{C_b}{H_L}\right)^{0.09} \quad \text{Eq. 12}$$

380   From the Eq. 12, one should note the small power coefficient for C_b/H_L, reflecting the slight

381   influence of this dimensionless number on expansion rate in the specific experimental area of

382   the study. This result confirmed the observations discussed previously. The agitation speed

383   has the major influence as Reynolds number has the highest coefficient value. From Eq. 12

384   and definitions of Re and Θ_m, the separate effects of agitation speed N and mixing time t_m can

385   be appreciated. Indeed, the latter physical quantity only appears in Θ_m value. On the other

386   hand, rotational speed is implicated in both dimensionless numbers. As a result, the expansion

387   rate could be viewed as approximately proportional to $N^{3/2}t_m^{1/2}$, in the studied intermediate

388   domain.

389   The same approach of modelling was then conducted for the turbulent regime ($Re > 10^5$).

390   Considering this regime, foam volume is a decreasing function of the Re number, due to foam

391   collapse. From Table 1, the last 18 assays were used here to fit the Eq. 11 to the data and

392   identify the proper constants in such turbulent domain. Fig. 4b points out the correlation

393   between experimental data and predicted values through the use of the monomial equation:

394
$$\frac{H_F}{H_L} = 10^{6.25}Re^{-1.32}\Theta_m^{\ 0.28}\left(\frac{C_b}{H_L}\right)^{-0.06} \quad \text{Eq. 13}$$

395   In case of turbulent regime, the monomial form of the process law appears to be less accurate

396   than in case of intermediate regime ($R^2 = 0.82$). In the turbulent regime, the strong agitation

397   shears and breaks bubbles faster than their generation. As a result, foam collapses and final

398   volume decreases with increasing speed of agitation. As the processes interfere at a complex

399   level, it becomes arduous to describe precisely the evolution of foam volume. However, the

400   model still allows obtaining a first general understanding of the system. As for the

401   intermediate regime, the π-number related to bottom clearance is shown to have minor

402   influence on foam rate of expansion. On the other hand, the power coefficient for Reynolds

403   number is negative as observed from experimental results: an increase of Re results in a

404   decrease in foam volume. Mixing time number, Θ_m, has slightly less influence on foam

405   expansion rate in turbulent regime compared to the intermediate one, as its power coefficient

406   is a factor two lower. For this regime, and from definitions of Re and Θ_m, the expansion rate

407   is approximatively proportional to $N^{-1}t_m^{1/3}$, in the studied turbulent domain. This behavior

408   is far different from the intermediate regime, confirming the choice of separating the two

409   regimes for the modelling.

410   Both power laws obtained from dimensional analysis may be used for predicting, with a

411   certain accuracy, the final volume of foam produced, with specific operating conditions, for

412   SLES solutions. Master curves of foam heights for different Reynolds numbers and mixing

413   time numbers are presented in Figure 5. To plot these curves a grid was created with different

414   Re in the first row and different Θ_m numbers in the first column. For each couple of Re and

415   Θ_m in the measuring range, the foam height was calculated using Eq. 12 or Eq. 13. The master

416   curves were plotted by applying 3D map feature in Microsoft Excel 2016. The non-plotted

417   area at the bottom right of the graph correspond to a domain not covered in this study

418   (intermediate flow regime coupled to high mixing time number), but one could appreciate the

419   consistency between intermediate flow regime and turbulent regime investigated. This

420   interesting map could avoid experimental runs when a particular amount of foam is desired.

421

422   *4.3. Cases of the other surfactants for intermediate regime (10^4 < Re < 10^5)*

423   The experiments were also conducted in the intermediate flow regime (10^4 < Re < 10^5) for the

424   two other model surfactants, Tween 20 and Brij L23. Only this regime was investigated for

425   these two surfactants as previous results with SLES reveal that this regime was the most

426   efficient for increasing the foaming amount. The data were compared to those of SLES in the

427   same intermediate flow regime. As in the case of SLES, final rates of expansion showed a

428   maximum at Reynolds numbers close to 10^5 (data not shown). Experiments also revealed that

429   bottom clearance had minor influence on foam generation for both surfactants.

430   Likewise, the correlation fitting was performed for Tween 20 and Brij L23 separately, in this

431   intermediate regime. Although fewer experimental data were available, a monomial form was

432   found to be adequate to describe the process as well for the two surfactants, according to Eq. 9

433   (R^2 = 0.94 and 0.77, for Tween 20 and BrijL23 respectively). The resulting process

434   relationships are shown in Eq. 14 and Eq. 15. These equations can be compared to Eq. 12

435　obtained for SLES in the same intermediate flow regime ($10^4 < Re < 10^5$). Fig. 6 showed the

436　good agreement between predicted and experimental values. As discussed before, the

437　dimensionless number describing bottom clearance effect (C_b/H_L) had no significant influence

438　on final foam expansion rate, compared to Re and Θ_m. According to the power coefficients in

439　Eq. 12, Eq. 14 and Eq.15, in the intermediate flow regime ($10^4 < Re < 10^5$), Reynolds number

440　has globally a higher influence on foaming ability than Θ_m and C_b/H_L whatever the surfactant.

441　Tween 20: $\dfrac{H_F}{H_L} = 10^{-2.0} Re^{0.20} \Theta_m{}^{0.17} \left(\dfrac{C_b}{H_L}\right)^{0.003}$　Eq. 14

442　Brij L23: $\dfrac{H_F}{H_L} = 10^{-4.6} Re^{0.69} \Theta_m{}^{0.28} \left(\dfrac{C_b}{H_L}\right)^{0.02}$　　Eq. 15

443　The comparison of these three relationships to the literature is not simple because the few

444　other studies dealing with foaming in stirred tanks have been carried out in different

445　experimental domains: different vessel sizes (therefore different range of Reynolds numbers),

446　different impeller type, with gas sparging, without surfactant, etc, and most of them don't take

447　into account the effect of time (duration of agitation). However, we can noticed the

448　correlation proposed by Smith (Smith 1992) between gas hold-up and both Reynolds and

449　Froude numbers with a positive power coefficient (0.35) relative to both those dimensionless

450　numbers. If Fr number is proportional to Re^2 as in our study, the power coefficient to Re

451　number alone in Smith correlation become 1.05 which is very close to the one we obtained for

452　SLES (1.09, Eq.12).

453　To go further, and in view of direct comparison of surfactants, calculations were tried with a

454　similar set of exponent for the three different molecules. The set of exponent obtained with

455　SLES (Eq. 12) was employed as the reference and applied to experimental data of Tween 20

456　and Brij L23 in order to find a generalized process law of the form of Eq. 16:

457　$$\left(\dfrac{H_F}{H_L}\right) = \alpha_i \left[Re^{1.09} \Theta_m{}^{0.57} \left(\dfrac{C_b}{H_L}\right)^{0.09} \right]^{\beta_i} \text{ Eq. 16}$$

458　with α_i and β_i constants that only depend on surfactant.

459 As shown in Table 2, the correlations between experimental and predicted values using Eq.16

460 are similar to those obtained with Eq. 12, Eq. 14 and Eq. 15, giving a sense to Eq.16.

461 Therefore, this supports the assumption that Reynolds number and mixing time number

462 influence in a similar way the foaming ability of surfactants solutions in that intermediate

463 flow regime. Values of α_i and β_i obtained for each surfactant are reported in Table 2. The

464 difference in these coefficient values can be related to own properties of each amphiphilic

465 molecule. Namely, SLES, Tween 20 and Brij L23 have different equilibrium surface tension

466 properties such as CMC and γ_{eq} at the CMC values. Moreover, the dynamic adsorption

467 properties and surface viscoelasticity are known to play a major role in the formation and

468 stabilization of foam films (Pugh 2016). Surely, the signification of these coefficients needs to

469 be further investigated, but it was not the initial purpose of the present study.

470 From Eq. 16 and values in Table 2, master curves Θ_m-Re allowing to compare the three

471 surfactants in intermediate flow regime ($10^4 < Re < 10^5$) were plotted as explained for Fig.5.

472 These are presented in Fig. 7. SLES is globally better at foaming since it produces higher

473 amount of foam in the studied experimental domain. Tween 20 is a poor foaming agent in

474 these conditions whereas Brij L23 allows to produce slightly more foam.

475 In addition, the previous process law (Eq. 16) determined by dimensional analysis and

476 associated master curves (Fig. 7) allow to predict the foam expansion rate for 3 model

477 surfactants in the studied experimental domain, i.e. $3.10^4 < Re < 8.10^4$, $350 < \Theta_m < 10^4$ and

478 $0.2 < C_b/H_L < 1$. At particular agitation speed and mixing time, dimensionless numbers

479 involved in the foam generation process are known, and the final amount of foam can be

480 anticipated.

481

482 **5. Conclusion**

483   In the present work, 3 model surfactants solutions were foamed in a mechanically agitated

484   vessel according to different process parameters: agitation speed, agitation time and bottom

485   clearance. By using the dimensional analysis approach, the foam ability of each surfactant

486   expressed as foam expansion rate could be correlated with success to two dimensionless

487   numbers well known in mechanical mixing processes: the Reynolds number and the mixing

488   time number. Reynolds number was observed as mainly governing the amount of formed

489   foam.

490   On the contrary, clearance bottom (C_b/H_L) of the agitator was shown to have no influence for

491   the whole range of Reynolds covered in this study.

492   Thanks to the wide range of Reynolds number covered in this study, it was shown a clear

493   difference between the intermediate flow regime ($Re < 10^5$) and the turbulent ones ($Re > 10^5$)

494   leading to a different process law for each regime. Indeed, an increase of Reynolds number

495   leads to an increase of foam expansion rate in intermediate flow regime but to a decrease of it

496   in turbulent regime. In the intermediate flow regime, a general process relationships was

497   proposed which allowed to compare the three surfactants with each other. Master curves were

498   finally drawn showing that SLES is globally better at foaming than Tween 20 and Brij L23,

499   the latter producing slightly more foam. In addition, those curves can be used for helping to

500   predict final foam volumes in the studied experimental domain according to both

501   dimensionless numbers.

502   This study is a first step for a better understanding and a better control of the impact of

503   process parameters on foam ability. The next investigations should concern essentially two

504   directions. The first one should elucidate the signification of α_i and β_i constants of the

505   generalized law by varying the parameters relative to surfactants solutions and maybe adding

506   new ones such as dynamic surface tension or surface viscoelasticity. As nothing guarantees

507   that the process relationship can be written in a monomial form, or is able to adjust to the

508 "true" physical laws (which are theoretical but analytically inaccessible), second prospect of

509 this work will concern the use of other mathematical functions than monomial one in order to

510 enhance the general fit and thus provide new insights about the way the process and the

511 surfactants parameters could be involved.

512

Acknowledgements

519

References

521

522 C. André, J. F. Demeyre, C. Gatumel, H. Berthiaux and G. Delaplace (2012). "Dimensional
523 analysis of a planetary mixer for homogenizing of free flowing powders: Mixing time and
524 power consumption." *Chemical Engineering Journal* **198-199**: 371-378 DOI:
525 http://doi.org/10.1016/j.cej.2012.05.069.

526 J. J. Bikerman (1973). Measurements of Foaminess. Foams. Springer-Verlag, Springer-Verlag
527 New York**:** 65-97.

528 M. M. Camacho, N. Martínez-Navarrete and A. Chiralt (1998). "Influence of locust bean
529 gum/λ-carrageenan mixtures on whipping and mechanical properties and stability of dairy
530 creams." *Food Research International* **31**(9): 653-658 DOI: http://doi.org/10.1016/S0963-
531 9969(99)00041-1.

532 A. Celani, S. Blackburn, M. J. H. Simmons and E. H. Stitt (2018). "Effect of mixing
533 conditions on the wet preparation of ceramic foams." *Chemical Engineering Research and
534 Design* **134**: 1-14 DOI: https://doi.org/10.1016/j.cherd.2018.03.044.

535 A. K. S. Chesterton, D. A. P. de Abreu, G. D. Moggridge, P. A. Sadd and D. I. Wilson (2013).
536 "Evolution of cake batter bubble structure and rheology during planetary mixing." *Food and
537 Bioproducts Processing* **91**(3): 192-206 DOI: http://doi.org/10.1016/j.fbp.2012.09.005.

538 V. Cristini and Y.-C. Tan (2004). "Theory and numerical simulation of droplet dynamics in
539 complex flows - A review." *Lab on a chip* **4**: 257-264 DOI: http://doi.org/10.1039/b403226h.

G. Delaplace, P. Coppenolle, J. Cheio and F. Ducept (2012). "Influence of whip speed ratios on the inclusion of air into a bakery foam produced with a planetary mixer device." *Journal of Food Engineering* **108**(4): 532-540 DOI: http://doi.org/10.1016/j.jfoodeng.2011.08.026.

G. Delaplace, Y. Gu, M. Liu, R. Jeantet, J. Xiao and X. D. Chen (2018). "Homogenization of liquids inside a new soft elastic reactor: Revealing mixing behavior through dimensional analysis." *Chemical Engineering Science* **192**: 1071-1080 DOI: http://doi.org/10.1016/j.ces.2018.08.023.

G. Delaplace, R. Guérin and J. C. Leuliet (2005). "Dimensional analysis for planetary mixer: Modified power and Reynolds numbers." *AIChE Journal* **51**(12): 3094-3100 DOI: http://doi.org/10.1002/aic.10563.

G. Delaplace, K. Loubière, F. Ducept and R. Jeantet (2015). Dimensional Analysis of Food Process, ISTE Press.

G. Delaplace, R. K. Thakur, L. Bouvier, C. André and C. Torrez (2007). "Dimensional analysis for planetary mixer: Mixing time and Reynolds numbers." *Chemical Engineering Science* **62**(5): 1442-1447 DOI: http://doi.org/10.1016/j.ces.2006.11.039.

G. Delaplace, C. Torrez, J. C. Leuliet, N. Belaubre and C. Andre (2001). "Experimental and CFD Simulation of Heat Transfer to Highly Viscous Fluids in an Agitated Vessel Equipped With a non Standard Helical Ribbon Impeller." *Chemical Engineering Research and Design* **79**(8): 927-937 DOI: https://doi.org/10.1205/02638760152721460.

P. Ding, S. Bakalis and Z. Zhang (2019). "Foamability in high viscous non-Newtonian aqueous two-phase systems composed of surfactant and polymer." *Colloids and Surfaces A: Physicochemical and Engineering Aspects* **582**: 123817 DOI: https://doi.org/10.1016/j.colsurfa.2019.123817.

W. Drenckhan and A. Saint-Jalmes (2015). "The science of foaming." *Advances in Colloid and Interface Science* **222**: 228-259 DOI: http://doi.org/10.1016/j.cis.2015.04.001.

S. M. Hall (2018). Chapter 6 - Blending and Agitation. Rules of Thumb for Chemical Engineers, 6t[h] edition. S. M. Hall, Elsevier**:** 99-124.

W. Hanselmann and E. Windhab (1998). "Flow characteristics and modelling of foam generation in a continuous rotor/stator mixer." *Journal of Food Engineering* **38**(4): 393-405 DOI: http://doi.org/10.1016/S0260-8774(98)00129-0.

R. Hassan, K. Loubiere, J. Legrand and G. Delaplace (2012). "A consistent dimensional analysis of gas–liquid mass transfer in an aerated stirred tank containing purely viscous fluids with shear-thinning properties." *Chemical Engineering Journal* **184**: 42-56 DOI: https://doi.org/10.1016/j.cej.2011.12.066.

C. Hsu and Y. F. Maa (1996). "Microencapsulation reactor scale-up by dimensional analysis." *Journal of Microencapsulation* **13**(1): 53-66 DOI: 10.3109/02652049609006803.

B. Hu, A. W. Nienow and A. W. Pacek (2003). "The effect of sodium caseinate concentration and processing conditions on bubble sizes and their break-up and coalescence in turbulent, batch air/aqueous dispersions at atmospheric and elevated pressures." *Colloids and Surfaces B: Biointerfaces* **31**(1): 3-11 DOI: https://doi.org/10.1016/S0927-7765(03)00038-9.

L. Indrawati, Z. Wang, G. Narsimhan and J. Gonzalez (2008). "Effect of processing parameters on foam formation using a continuous system with a mechanical whipper." *Journal of Food Engineering* **88**(1): 65-74 DOI: https://doi.org/10.1016/j.jfoodeng.2008.01.015.

E. Jakubczyk and K. Niranjan (2006). "Transient development of whipped cream properties." *Journal of Food Engineering* **77**(1): 79-83 DOI: http://doi.org/10.1016/j.jfoodeng.2005.06.046.

P. Kanokkarn, T. Shiina, M. Santikunaporn and S. Chavadej (2017). "Equilibrium and dynamic surface tension in relation to diffusivity and foaming properties: Effects of surfactant type and structure." *Colloids and Surfaces A: Physicochemical and Engineering Aspects* **524**: 135-142 DOI: http://doi.org/10.1016/j.colsurfa.2017.04.043.

A. Kroezen, J. Groot Wassink and E. Bertlein (1988). Foam Generation in a Rotor-Stator Mixer.

K. Lachin, C. Turchiuli, V. Pistre, G. Cuvelier, S. Mezdour and F. Ducept (2020). "Dimensional analysis modeling of spraying operation – Impact of fluid properties and pressure nozzle geometric parameters on the pressure-flow rate relationship." *Chemical Engineering Research and Design* **163**: 36-46 DOI: https://doi.org/10.1016/j.cherd.2020.08.004.

V. Machon, A. W. Pacek and A. W. Nienow (1997). "Bubble Sizes in Electrolyte and Alcohol Solutions in a Turbulent Stirred Vessel." *Chemical Engineering Research and Design* **75**(3): 339-348 DOI: https://doi.org/10.1205/026387697523651.

P. Manjula, P. Kalaichelvi and K. Dheenathayalan (2010). "Development of mixing time correlation for a double jet mixer." *Journal of Chemical Technology & Biotechnology* **85**(1): 115-120 DOI: http://doi.org/10.1002/jctb.2274.

G. Mary, S. Mezdour, G. Delaplace, R. Lauhon, G. Cuvelier and F. Ducept (2013). "Modelling of the continuous foaming operation by dimensional analysis." *Chemical Engineering Research and Design* **91**(12): 2579-2586 DOI: http://doi.org/10.1016/j.cherd.2013.05.020.

A. H. Massey, A. S. Khare and K. Niranjan (2001). "Air Inclusion Into a Model Cake Batter Using a Pressure Whisk: Development of Gas Hold-up and Bubble Size Distribution." *Journal of Food Science* **66**: 1152-1157 DOI: http://doi.org/10.1111/j.1365-2621.2001.tb16097.x.

J. Medek and I. Fořt (1979). "Pumping effect of impellers with flat incined blades." *Collection of Czechoslovak Chemical Communications* **44**: 3078-3089 DOI: http://doi.org/10.1135/cccc19793077.

A. Mohanan, M. T. Nickerson and S. Ghosh (2020). "Utilization of pulse protein-xanthan gum complexes for foam stabilization: The effect of protein concentrate and isolate at various pH." *Food Chemistry* **316**: 126282 DOI: https://doi.org/10.1016/j.foodchem.2020.126282.

N. Müller-Fischer and E. J. Windhab (2005). "Influence of process parameters on microstructure of food foam whipped in a rotor–stator device within a wide static pressure range." *Colloids and Surfaces A: Physicochemical and Engineering Aspects* **263**(1): 353-362 DOI: https://doi.org/10.1016/j.colsurfa.2004.12.057.

N. Müller, D. Suppiger and E. Windhab (2007). "Impact of Static Pressure and Volumetric Energy Input on the Microstructure of Food Foam Whipped in a Rotor-Stator Device." *Journal of Food Engineering* **80**: 306-316 DOI: http://doi.org/10.1016/j.jfoodeng.2006.05.026.

N. Müller, P. Tobler, M. Dressler, P. Fischer and E. Windhab (2008). "Single bubble deformation and breakup in simple shear flow." *Experiments in Fluids* **45**(5): 917-926 DOI: http://doi.org/10.1007/s00348-008-0509-1.

629 S. Nagata, M. Yanagimoto and T. Yokoyama (1957). "A Study on the Mixing of High-
630 viscosity Liquid." *Chemical engineering* **21**(5): 278-286 DOI:
631 https://doi.org/10.1252/kakoronbunshu1953.21.278.

632 A. Patist, S. S. Bhagwat, K. W. Penfield, P. Aikens and D. O. Shah (2000). "On the
633 measurement of critical micelle concentrations of pure and technical-grade nonionic
634 surfactants." *Journal of Surfactants and Detergents* **3**(1): 53-58 DOI:
635 http://dx.doi.org/10.1007/s11743-000-0113-4.

636 D. Pradilla, W. Vargas and O. Alvarez (2015). "The application of a multi-scale approach to
637 the manufacture of concentrated and highly concentrated emulsions." *Chemical Engineering*
638 *Research and Design* **95**: 162-172 DOI: http://doi.org/10.1016/j.cherd.2014.10.016.

639 R. J. Pugh (2016). Bubble and Foam Chemistry, Cambridge University Press.

640 M. J. Rosen, Y.-P. Zhu and S. W. Morrall (1996). "Effect of Hard River Water on the Surface
641 Properties of Surfactants." *Journal of Chemical & Engineering Data* **41**(5): 1160-1167 DOI:
642 http://dx.doi.org/10.1021/je960134l.

643 K. Samaras, M. Kostoglou, T. D. Karapantsios and P. Mavros (2014). "Effect of adding
644 glycerol and Tween 80 on gas holdup and bubble size distribution in an aerated stirred tank."
645 *Colloids and Surfaces A: Physicochemical and Engineering Aspects* **441**: 815-824 DOI:
646 https://doi.org/10.1016/j.colsurfa.2013.02.031.

647 E. Santini, E. Jarek, F. Ravera, L. Liggieri, P. Warszynski and M. Krzan (2019). "Surface
648 properties and foamability of saponin and saponin-chitosan systems." *Colloids and Surfaces*
649 *B: Biointerfaces* **181**: 198-206 DOI: https://doi.org/10.1016/j.colsurfb.2019.05.035.

650 J. M. Smith (1992). Simple Performance Correlations for Agitated Vessels. Fluid Mechanics
651 of Mixing: Modelling, Operations and Experimental Techniques. R. King. Dordrecht,
652 Springer Netherlands**:** 55-63, DOI: https://doi.org/10.1007/1978-1094-1015-7973-1005_1007.

653 H. A. Stone (2003). "Dynamics of Drop Deformation and Breakup in Viscous Flows." *Annual*
654 *Review of Fluid Mechanics* **26**(1): 65-102 DOI:
655 http://doi.org/10.1146/annurev.fl.26.010194.000433.

656 T. Szirtes and P. Rózsa (2007). Applied Dimensional Analysis and Modeling. Burlington,
657 Butterworth-Heinemann.

658 Z. Wang, F. Liu, Q. Zhang, X. Wei, D. Sun, G. Li and G. Zhang (2005). "Adsorption kinetics
659 of Brij 35 at air/solution interface." *Indian Journal of Chemistry - Section A Inorganic,*
660 *Physical, Theoretical and Analytical Chemistry* **44**(10): 2051-2054,
661 https://www.scopus.com/inward/record.uri?eid=2-s2.0-
662 28244477560&partnerID=40&md5=3fe4e8028a2439ee0a1d7132a95f959c.

663 F. White (2001). Fluid Mechanics, 7th edition, McGraw-Hill.

664 C. Wu, K. Nesset, J. Masliyah and Z. Xu (2012). "Generation and characterization of
665 submicron size bubbles." *Advances in Colloid and Interface Science* **179-182**: 123-132 DOI:
666 http://doi.org/10.1016/j.cis.2012.06.012.

667 J. Zhu, Z. Qian, M. Eid, F. Zhan, M. A. Ismail, J. Li and B. Li (2021). "Foaming and
668 rheological properties of hydroxypropyl methylcellulose and welan gum composite system:
669 The stabilizing mechanism." *Food Hydrocolloids* **112**: 106275 DOI:
670 https://doi.org/10.1016/j.foodhyd.2020.106275.

671 M. Zlokarnik (1998). "Problems in the application of dimensional analysis and scale-up of
672 mixing operations." *Chemical Engineering Science* **53**(17): 3023-3030 DOI:
673 http://doi.org/10.1016/S0009-2509(98)00131-6.

674

Fig. 1. Illustration of a foam generation process through mechanical agitation, and physical numbers involved in the amount of created foam H_F.

Fig. 2. Evolution of foam expansion rate for SLES solution with C_b/H_L ratio, for different agitation speeds and times. Lines used as guide only.

Fig. 3. (a) Evolution of foam expansion rate with Reynolds number, for various mixing times for SLES solution. Stirring element is at the air-liquid interface ($C_b=H_L$). (b) Evolution of foam expansion rate with mixing time number (Θ_m), for different agitation speeds. Stirring element is at the air-liquid interface ($C_b=H_L$). Lines used as guide only.

Fig. 4. (a) Correlation between experimental H_F/H_L in intermediate flow regime ($Re < 10^5$) and predicted ones using Eq.12 for SLES solution. (b) Correlation between experimental H_F/H_L in turbulent regime ($Re > 10^5$) and predicted ones using Eq.13 for SLES solution 8.

Fig. 5. Master curves of H_F/H_L of SLES solution as a function of Reynolds number and mixing time number, as predicted by Eq.12 and Eq.13.
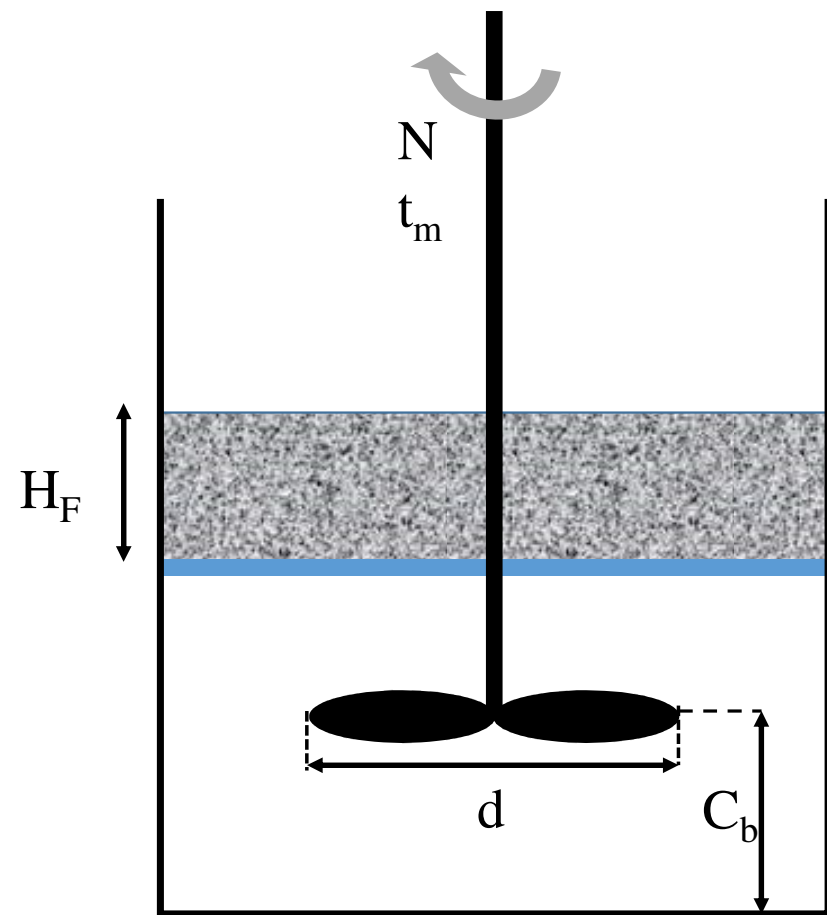
Fig. 6. Results of data modelling from Equations 14 and 15 for foam expansion rate of (a) Tween 20 and (b) BrijL23, in the intermediate flow regime; experimental domain of validity: $3.10^4 < Re < 8.10^4$, $350 < \Theta_m < 10^4$ and $0.2 < C_b/H_L < 1$.
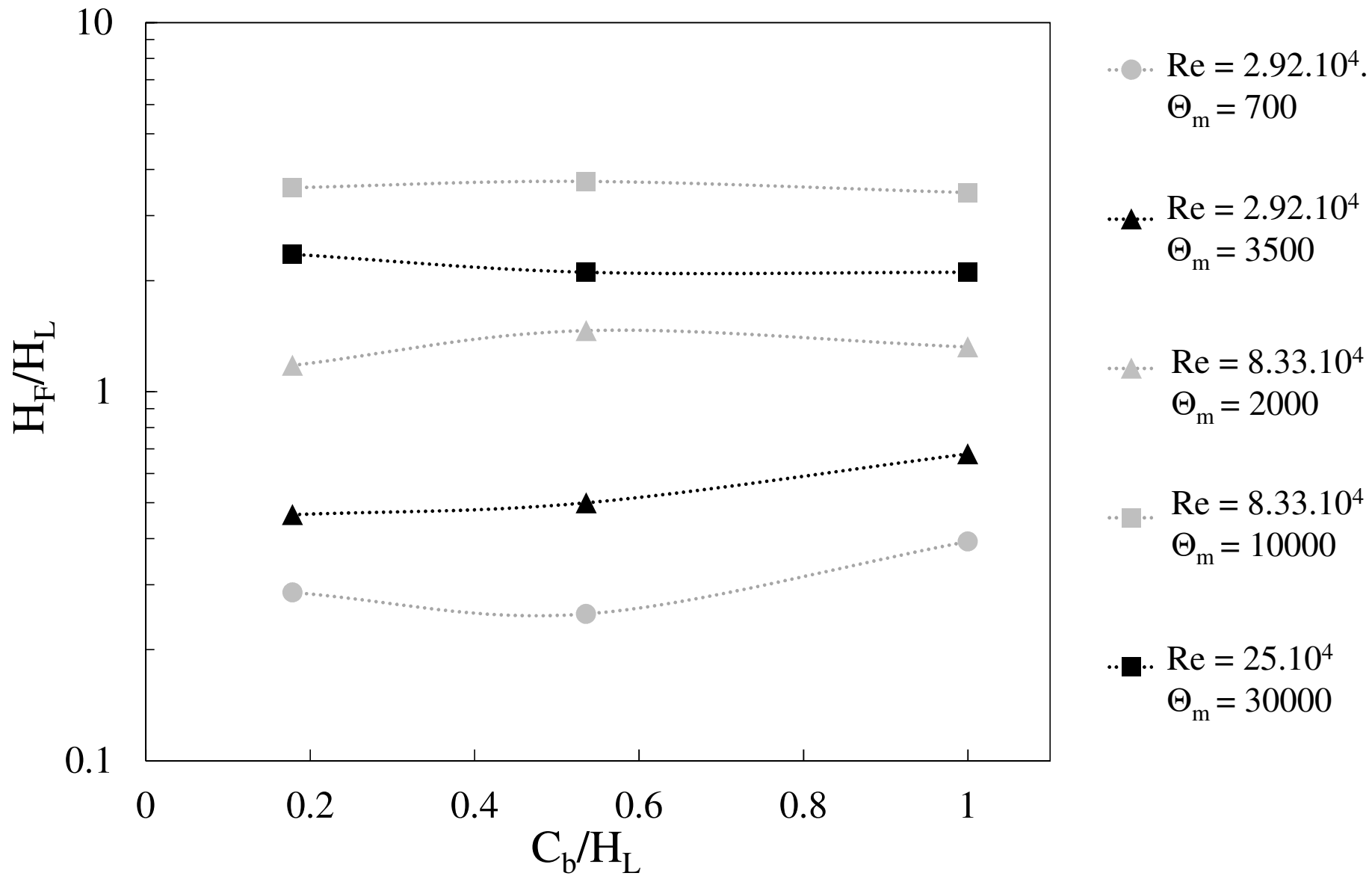
Fig. 7. Master curves of foam rate of expansion as a function of Reynolds number and mixing time number, as predicted by Eq.16 for (a) SLES, (b) Tween 20 and (c) Brij L23, in the intermediate flow regime; experimental domain of validity: $3.10^4 < Re < 8.10^4$, $350 < \Theta_m < 10^4$ and $0.2 < C_b/H_L < 1$.

Surfactant solution
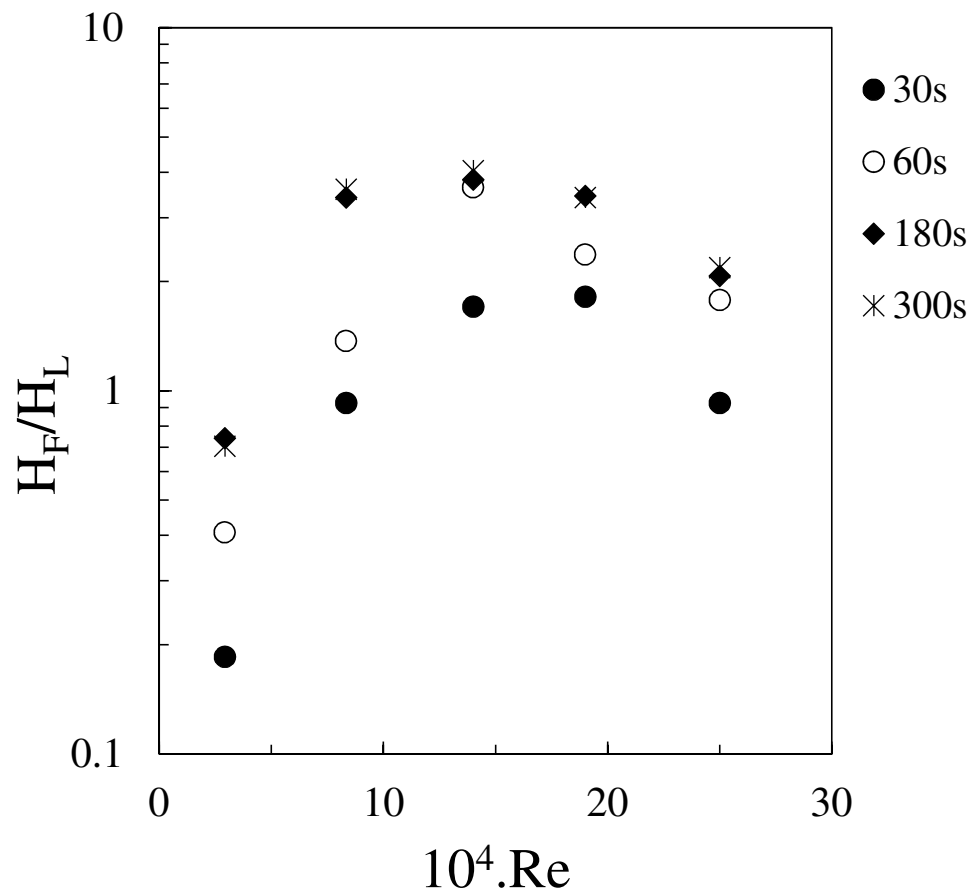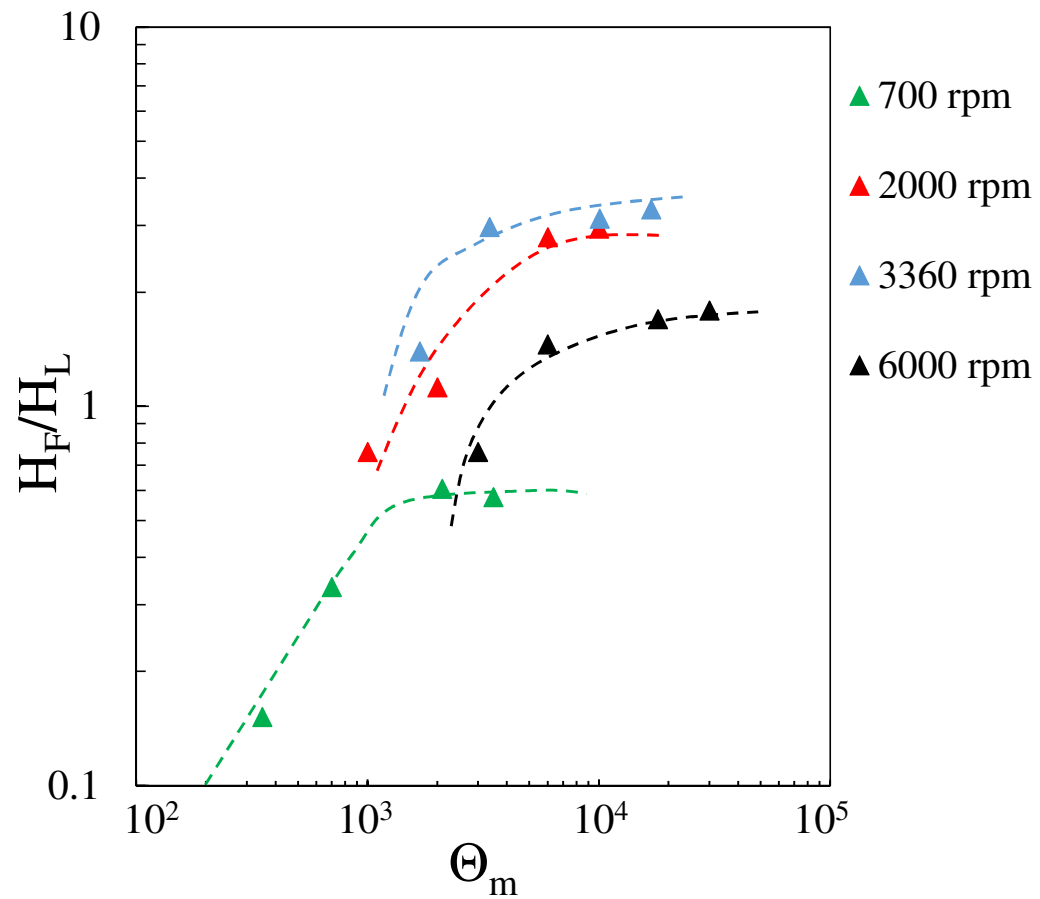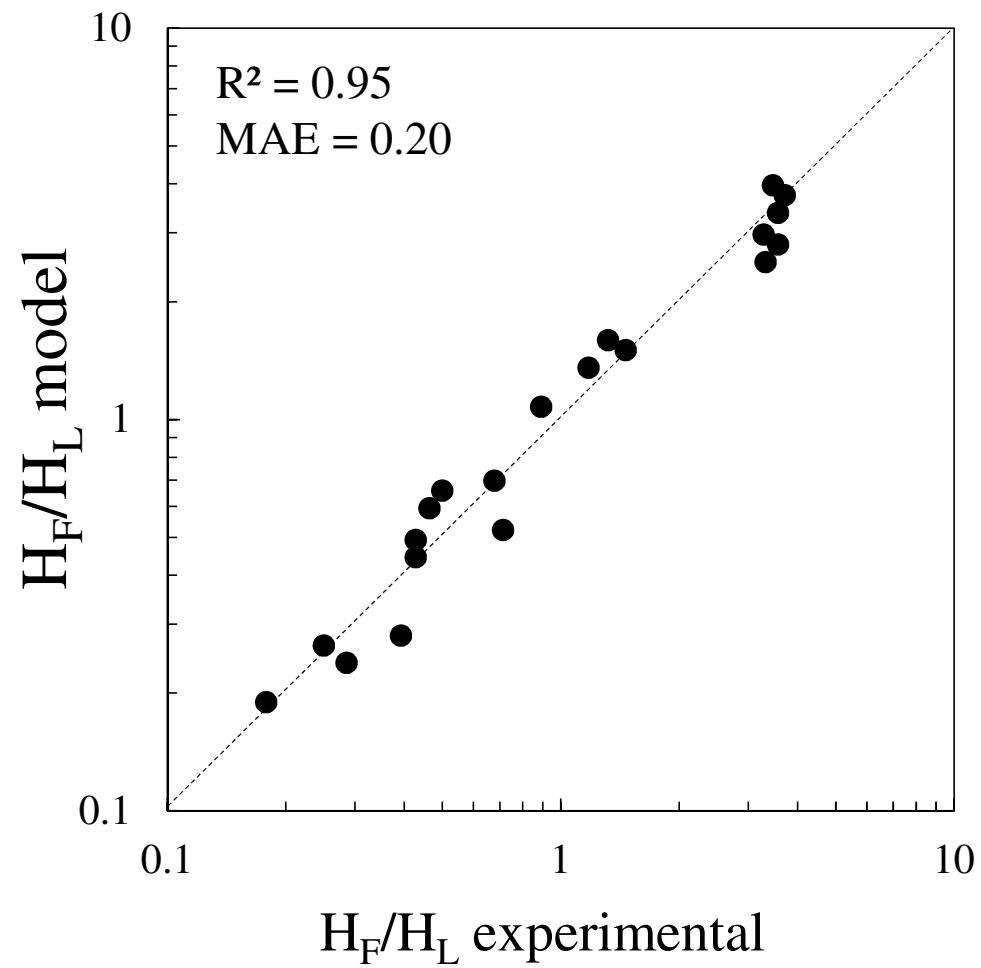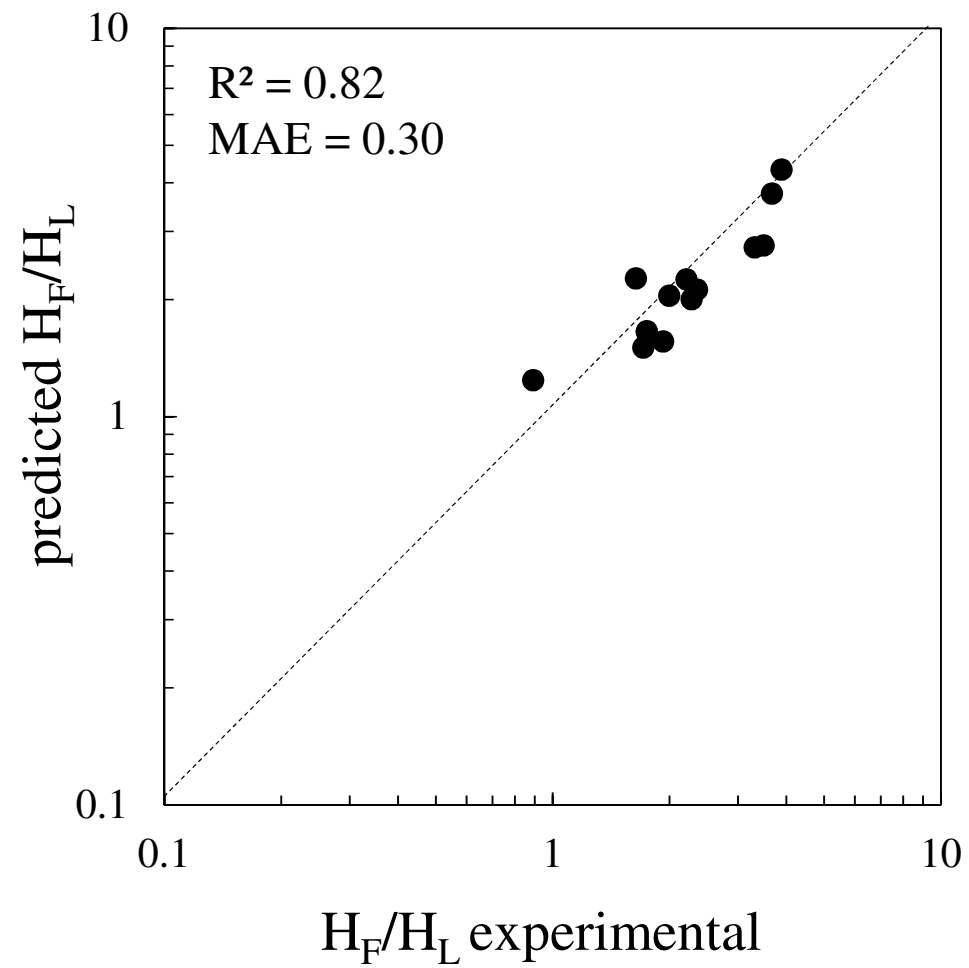ρ, η, γ

H_L

T

g
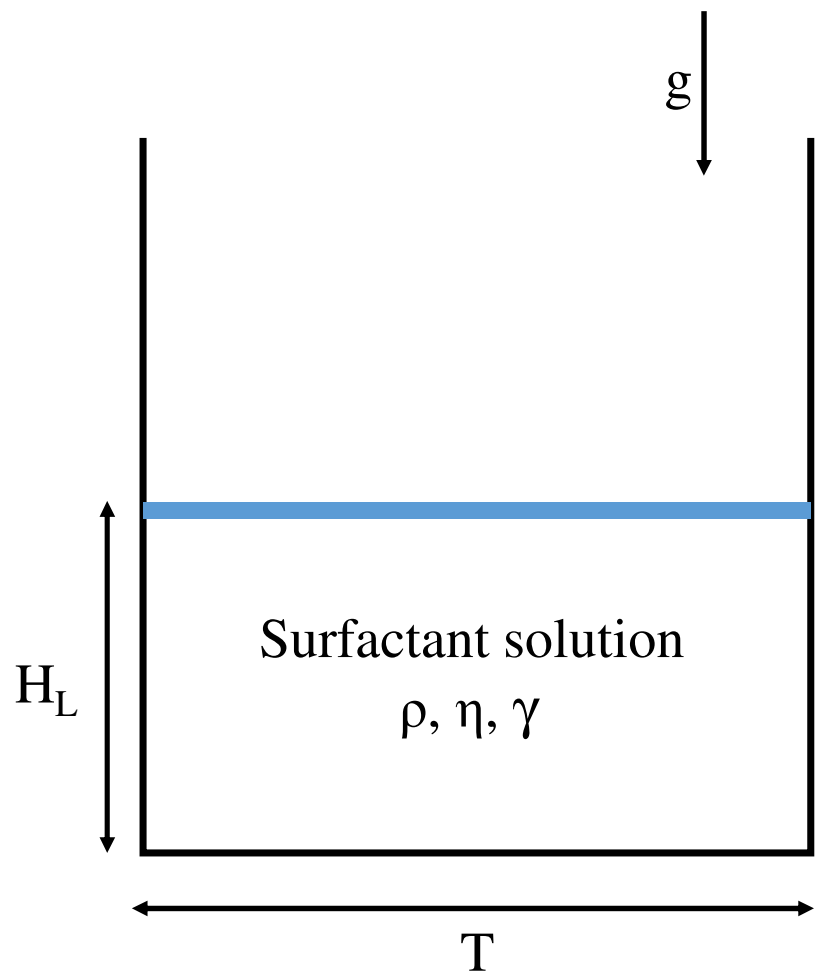
Mechanical shearing

(N, t_m)

N
t_m

H_F

d

C_b

(a)

(b)

(a)

(b)

(a)

(b)

(a)

$H_F/H_L = 4$

$H_F/H_L = 3$

$H_F/H_L = 2$

$H_F/H_L = 1$

10^4 Re

7.0

5.0

3.0

Θ_m

0   2000   4000   6000   8000   10000

(b)

$H_F/H_L = 0.3$

$H_F/H_L = 0.4$

10^4 Re

7.0

5.0

3.0

Θ_m

0   2000   4000   6000   8000   10000

(c)

$H_F/H_L = 0.8$

$H_F/H_L = 0.4$

10^4 Re

7.0

5.0

3.0

Θ_m

0   2000   4000   6000   8000   10000
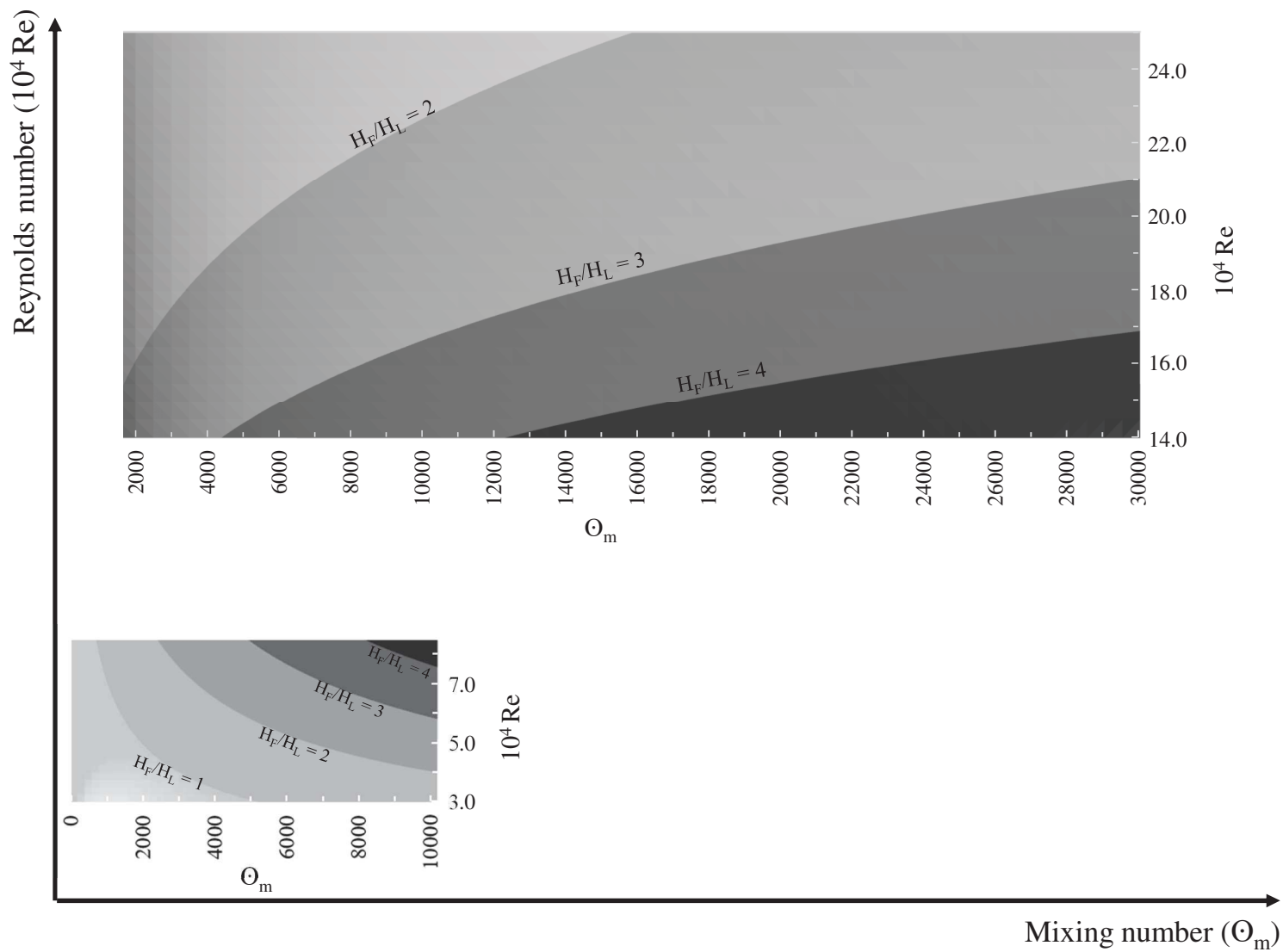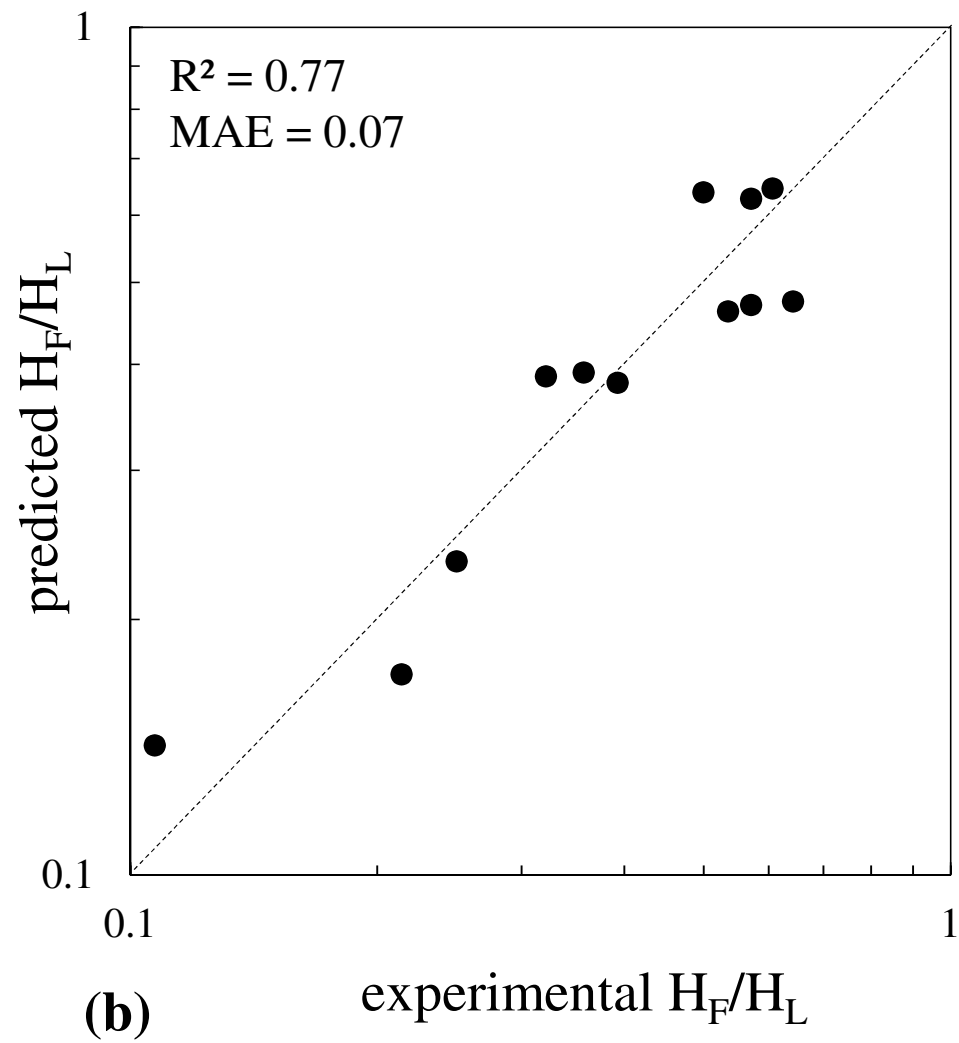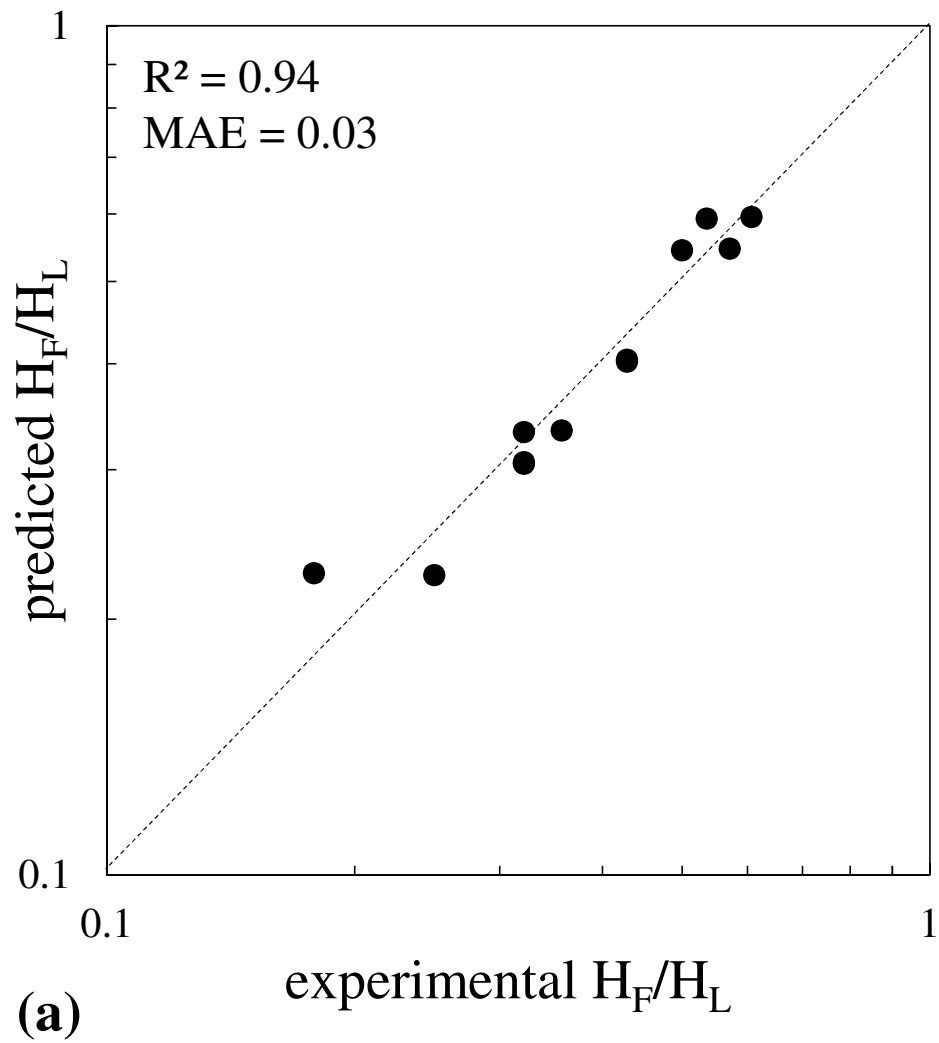
Table 1. Foaming trials settings and experimental values of H_F, for aqueous solutions of SLES (d/H_L=1.79 and T/H_L=3.21).

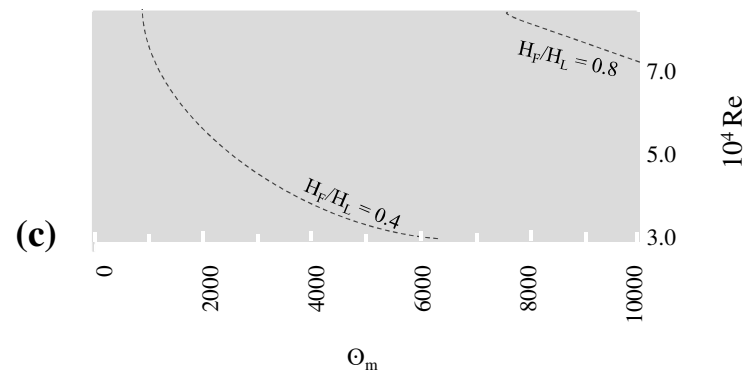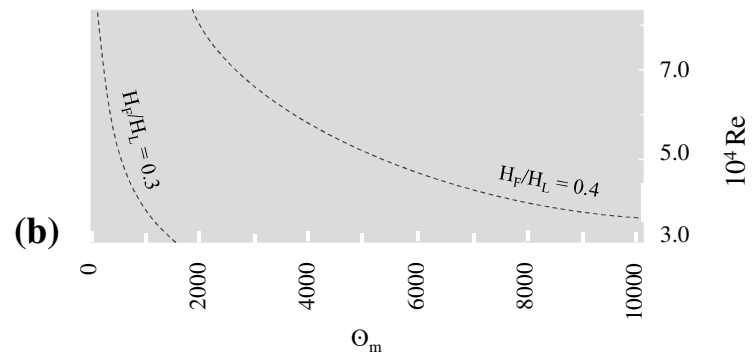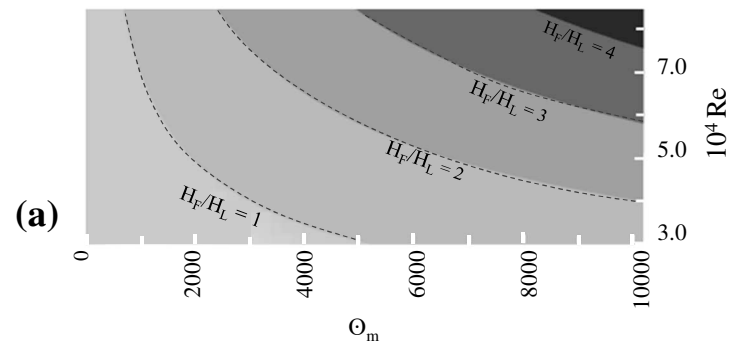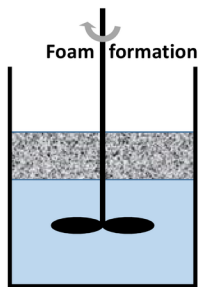| Trial	Physical quantities				Dimensionless numbers				
	N (rpm)	t_m (s)	C_b (m)	H_F (m)	Re /10^4	Ca	Θ_m	C_b/H_L	H_F/H_L
1	700	30	0.028	0.005	2.92	0.02	350	1.0	0.18
2	700	60	0.005	0.008	2.92	0.02	700	0.2	0.29
3	700	60	0.015	0.007	2.92	0.02	700	0.5	0.25
4	700	60	0.028	0.011	2.92	0.02	700	1.0	0.39
5	700	180	0.005	0.012	2.92	0.02	2100	0.2	0.43
6	700	180	0.015	0.012	2.92	0.02	2100	0.5	0.43
7	700	180	0.028	0.020	2.92	0.02	2100	1.0	0.71
8	700	300	0.005	0.013	2.92	0.02	3500	0.2	0.46
9	700	300	0.015	0.014	2.92	0.02	3500	0.5	0.50
10	700	300	0.028	0.019	2.92	0.02	3500	1.0	0.68
11	2000	30	0.028	0.025	8.33	0.06	1000	1.0	0.89
12	2000	60	0.005	0.033	8.33	0.06	2000	0.2	1.18
13	2000	60	0.015	0.041	8.33	0.06	2000	0.5	1.46
14	2000	60	0.028	0.037	8.33	0.06	2000	1.0	1.32
15	2000	180	0.005	0.093	8.33	0.06	6000	0.2	3.32
16	2000	180	0.015	0.100	8.33	0.06	6000	0.5	3.57
17	2000	180	0.028	0.092	8.33	0.06	6000	1.0	3.29
18	2000	300	0.005	0.100	8.33	0.06	10000	0.2	3.57
19	2000	300	0.015	0.104	8.33	0.06	10000	0.5	3.71
20	2000	300	0.028	0.097	8.33	0.06	10000	1.0	3.46
21	3360	30	0.028	0.046	14.0	0.10	1680	1.0	1.64
22	3360	60	0.028	0.098	14.0	0.10	3360	1.0	3.50
23	3360	180	0.028	0.103	14.0	0.10	10080	1.0	3.68
24	3360	300	0.028	0.109	14.0	0.10	16800	1.0	3.89
25	4560	30	0.028	0.049	19.0	0.13	2280	1.0	1.75
26	4560	60	0.028	0.064	19.0	0.13	4560	1.0	2.29
27	4560	180	0.028	0.093	19.0	0.13	13680	1.0	3.32
28	4560	300	0.028	0.092	19.0	0.13	22800	1.0	3.29
29	6000	30	0.028	0.025	25.0	0.17	3000	1.0	0.89
30	6000	60	0.028	0.048	25.0	0.17	6000	1.0	1.71
31	6000	60	0.015	0.054	25.0	0.17	6000	0.5	1.93
32	6000	60	0.005	0.049	25.0	0.17	6000	0.2	1.75
33	6000	180	0.028	0.056	25.0	0.17	18000	1.0	2.00
34	6000	180	0.015	0.066	25.0	0.17	18000	0.5	2.36
35	6000	180	0.005	0.062	25.0	0.17	18000	0.2	2.21
36	6000	300	0.028	0.059	25.0	0.17	30000	1.0	2.11
37	6000	300	0.015	0.059	25.0	0.17	30000	0.5	2.11
38	6000	300	0.005	0.066	25.0	0.17	30000	0.2	2.36

Table 2. Constants from equation 11, R^2 and MAE for each surfactant

Surfactant	α_i	β_i	R^2 (MAE)
SLES	10^{-7}	1.0	0.95 (0.20)
Tween 20	$8.60 \cdot 10^{-3}$	0.23	0.95 (0.02)
Brij L23	$3.78 \cdot 10^{-5}$	0.57	0.71 (0.07)

Prediction of foam volume

Foam formation

$$\frac{H_F}{H_L} = Const. \, Re^a \, Ca^b \, \Theta_m{}^c \left(\frac{C_b}{H_L}\right)^d$$

$R^2 = 0.95$
MAE = 0.20

Experimental part · Dimensional analysis